JOM
https://doi.org/10.1007/s11837-019-03750-y

Inverse Simulation of Fracture Parameters for Cement-Bonded Corundum Refractories

LIPING PAN,[1,2] ZHU HE,[1,2,4] YAWEI LI,[1,2,5] BAOKUAN LI,[1,2] and SHENGLI JIN[3]

1.—The State Key Laboratory of Refractories and Metallurgy, Wuhan University of Science and Technology, Wuhan 430081, China. 2.—National-provincial Joint Engineering Research Center of High Temperature Materials and Lining Technology, Wuhan University of Science and Technology, Wuhan 430081, China. 3.—Chair of Ceramics, Montanuniversitaet, Peter-Tunner Strasse 5, 8700 Leoben, Austria. 4.—e-mail: hezhu@wust.edu.cn. 5.—e-mail: liyawei@wust.edu.cn

In order to obtain the real solution of the fracture parameters for the wedge-splitting test, numerical simulation and inverse algorithm have been designed to estimate the maximum tensile stress and fracture energy of cement-bonded corundum refractory. The experimental and simulated curves have been systematically compared to produce the bilinear model of cohesive zone material with the inverse algorithm of nonlinear least-squares solution being the most suitable for the simulation of the wedge-splitting test. Furthermore, the inverse simulation procedure has been applied to specimens of various heating temperatures and cement contents. Consequently, the fracture energy and the maximum tensile stress initially decrease and then increase with the temperature. Furthermore, the fracture energy has the tendency of increasing with the cement content, and the maximum tensile stress has the highest peak at the content of 10 wt.%. Additionally, the cement-bonded corundum refractory presents higher brittleness after high-temperature heating (1400°C) or with the cement content of 10 wt.% at 110°C.

INTRODUCTION

Thermal shock during the service process of cement-bonded corundum refractories greatly shortens the service life. Hence, improving the thermal shock resistance of refractories is one of the most crucial factors that determine the material quality.[1–3] Usually, there are a few popular methods, such as the water-quenching method (PRE/RS-1), the air quenching method (PRE/RS-2), etc., that are used to measure the thermal resistance of refractories. These evaluation criteria utilize the attenuation of rupture strength to characterize the thermal shock resistance of materials, rather than depend on the quantitative parameters (e.g., fracture energy) of fracture mechanics. From the mechanical point of view, cement-bonded corundum refractories can be considered as a two-phase material made of a cement-based matrix composed of cement and fine corundum (min. powder size typically nm), and the coarse aggregates of corundum (max. grain size typically 3–5 mm).[4,5] Being a heterogeneous material, cement-bonded corundum refractories belong to the materials with congenital defects, which inevitably have various sizes of porosity and cracks after preparation.[6,7] Cracks initiate, propagate and penetrate, even causing instability and rupture of materials after several times of thermal shocking.[8] Furthermore, the linear elastic fracture theory is no longer appropriate to analyze the crack propagation of materials when the crack zone and subcritical propagation length at the crack end cannot be ignored.[9,10]

Tschegg[11] patented the wedge-splitting test (WST) in the 1980s, which can perform a stable fracture process based on a fictitious crack model.[12] The schematic of the WST is shown in Fig. 1a. A large block refractory specimen (1) is prepared, and the structure is formed by prefabricated grooves and crack channels of a certain size on part 1. A wedge block (2), two support blocks (3) and two transmission rollers (4) are added to part 1 in the experiment. By loading the vertical force F_V at a certain rate on part 2, a crack is formed in the prefabricated

Published online: 04 September 2019

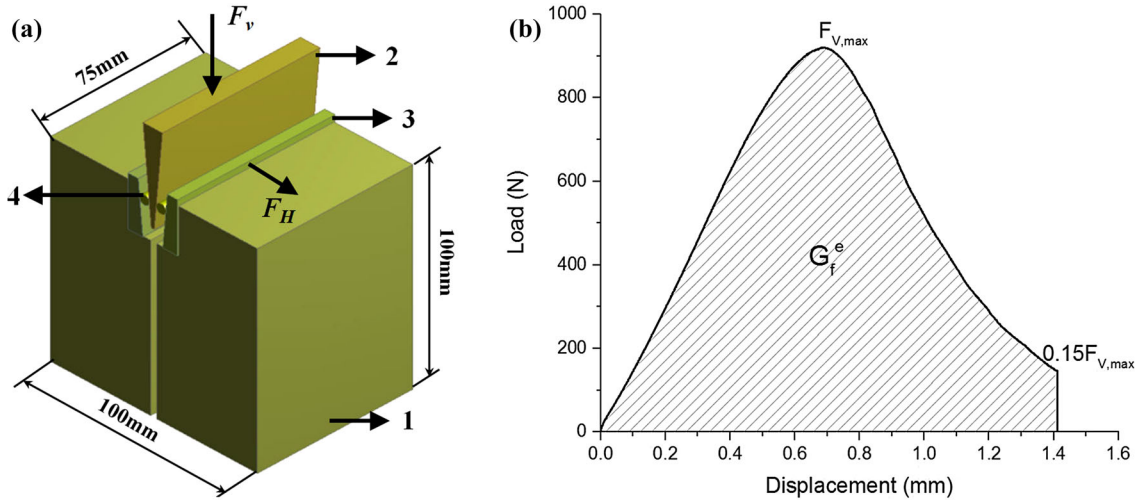

Fig. 1. (a) Schematic diagram of wedge-splitting experiment; *1* specimen of refractories, *2* wedge block *3* support block, *4* transmission roller. (b) Load–displacement curve.

crack channel, and the force–displacement curve shown in Fig. 1b is recorded. From the point of F_v, visible cracks appear on the grooves and propagate with the decline of the load. WST has proved to be a more effective and reliable way for determining the fracture properties of concrete,[13,14] and hence it is used for the refractory.[15–17] The fracture parameters including fracture energy can be calculated from the force–displacement curve.[13,18] Despite various good properties, the experiment is often stopped when the load reaches a certain value of the maximum (0.15 $F_{v,max}$; Fig. 1b) to ensure the safety of the equipment, resulting in an incomplete force–displacement curve and untrue solution of the fracture parameters.

Inverse analysis is proposed to determine the material properties, especially the fracture parameters including fracture energy, tensile strength, etc. After obtaining the force–displacement curves from the WST, the initial fracture parameters can be determined, and then the optimization process is conducted to minimize a suitable norm for discrepancies between the experimental data and the corresponding data obtained from the simulation. Roelfstra and Wittmann[19] proposed an algorithm for minimizing the deviation between the experimental and simulated load–displacement curves by using software, which was based on the finite element method and the discrete crack approach with a bilinear softening curve. This method is inefficient because it requires that the input parameter should be quite close to the literation results. Skocek[20] presented the hinge model for the WST of concrete, which can derive a closed-form analytical solution for the softening curve, but it was limited by the assumption that the plane sections were a certain distance from the crack path, because the specimens for the WST cannot always achieve this demand. Kitsutaka[21] used the poly-linear method, which included a step-by-step extension of the softening curve, and the following point on the softening curve was obtained by minimization of the difference between the computed and the measured loads corresponding to the investigated crack opening. Although it can be performed without any assumption, the relationship between load and displacement was heavily influenced by any measurement error at each point, and the previous errors can be accumulated. It can be concluded that the critical factors restricting the accuracy of the inverse analysis are the force–displacement relationship of the crack surface and the optimization algorithm. From previous works, the most commonly used method to fit the two results is the nonlinear least-squares solution (NL2SOL), which has the objective function and optimization algorithm within the program.[22] Combined with the cohesive zone material (CZM) model of the finite element method,[23,24] the fracture parameters can be calculated inversely. Nevertheless, few studies have been carried out to predict the fracture parameters of cement-bonded corundum refractories by inverse simulation. Therefore, an inverse simulation for the fracture parameters of WST for cement-bonded corundum refractories is proposed and tested in the present paper. The procedure takes the maximum tensile stress and fracture energy as the input optimization parameters, and the force–displacement curve obtained from the experiment as the output correction parameter. The inverse analysis is carried out by using the commercial finite element analysis software, ANSYS,and the optimization algorithm, NL2SOL. Consequently, the final mechanical parameters such as fracture energy, maximum tensile stress and characteristic length are compared to the experimental data for various types of specimens.

EXPERIMENTAL AND SIMULATION PROCEDURES

Experimental Procedure

The raw materials used for specimens were 70 wt.% tabular corundum (5–3 mm, 3–1 mm, 1–0 mm, 98.6 wt.% Al_2O_3; Zhejiang, China), 19 wt.% corundum powder (200 mesh and 325 mesh, 98.6 wt.% Al_2O_3; Zhejiang), and 6 wt.% aluminates powder ($\sim$ 2 μm, 99.02 wt.% Al_2O_3; Kaifeng, China). The calcium aluminate cement type Secar 71 ($\leq$ 50 μm, 70.47 wt.% Al_2O_3, 28.08 wt.% CaO; Lafarge, France) was used as the binder, while 4.5 wt.% water and 0.1 wt.% dispensing agent (FS60; BASF, Germany) were added to the compositions. The cement-bonded corundum refractories were shaped in wedge-splitting molds after mixing and cured under the conditions of 25°C and 75% humidity for 24 h, and dried at 110°C for 72 h. Finally, the as-prepared samples with various cement content (5 wt.%, 10 wt.% and 15 wt.%) were heated at 1100°C and 1400°C for 3 h, respectively, in which the heating rate was 5°C/min.

The WST was performed using a universal test machine (ETM 1050) with the maximum load capacity of 100 KN and speed of 0.5 mm/min at room temperature. To protect the equipment, the experiment procedure was stopped when the force reached 0.15 $F_{v,max}$, and the force–displacement curves were recorded correspondingly. The fracture energy, G_f^E, and maximum tensile stress, σ_{max}^E, can be determined from the force–displacement experimental curves using the following formulae:[11]

$$G_f^E = \frac{1}{A}\int_0^{X_V} F_V dX \tag{1}$$

where A is the projection area of the fracture surface and F_V and X_V present the vertical load and displacement, respectively.

$$\sigma_{max}^E = \frac{F_{H,max}}{bh}\left(1+\frac{6z}{h}\right) \tag{2}$$

where F_H denotes the horizontal load of the crack surface, b and h are the thickness and the height of the crack surface, respectively, and z is the vertical distance between the center of gravity of the fracture surface and the horizontal force.

Another fracture parameter of the characteristic length, l_{ch}^E,[11] is calculated as follows, which characterizes the sensitivity of materials against crack propagation:

$$l_{ch}^E = \frac{G_f^E \cdot E}{\sigma_{max}^{E\,2}} \tag{3}$$

where E represents the elasticity modulus, which is determined by the resonance frequency dynamic method using an elastic modulus and damping analyzer (RFDA-HT1600; IMCE, Belgium) at room temperature.

Simulation Procedure

The numerical simulation and the inverse algorithm are used to determine the accurate fracture parameters. The CZM model between the stress acting on the interface and the corresponding interfacial separation have been chosen to simulate the crack propagation. The inversed algorithm is conducted to achieve fracture parameters such as fracture energy and maximum tensile stress by using the commercial finite element analysis software and the optimization algorithm, NL2SOL.

Different CZM models can be selected for various materials, e.g., bilinear, trapezoidal, exponential and polynomial force–displacement relationships. The exponential law is widely used to simulate the interface fracture behavior of composites and the bilinear law is the most efficient method and extensively adopted for a wide range of materials.

An exponential form of the CZM model, originally proposed by Xu and Needleman, uses the surface fracture energy:[25]

$$\phi(\delta_n) = e\sigma_{max}\delta_n^*[1-(1+\Delta_n)e^{-\Delta_n}] \tag{4}$$

where $\phi(\delta_n)$ is the surface fracture energy, δ_n is the normal separation displacement, e is the natural logarithmic constant, σ_{max} is the maximum tensile stress at the interface, δ_n^* is the normal separation displacement across the interface when the maximum tensile stress is attained, and Δ_n is the ratio of δ_n and δ_n^*.

The tensile stress is defined as:

$$\sigma = \frac{\partial\phi(\delta_n)}{\partial\delta_n} \tag{5}$$

From Eqs. 4 and 5, the tensile stress of the interface is obtained:

$$\sigma = e\sigma_{max}\Delta_n e^{-\Delta_n} \tag{6}$$

For the exponential CZM model, the fracture energy, G_f, is expressed as:

$$G_f = e \times \sigma_{max} \times \delta_n^* \tag{7}$$

The bilinear CZM model, which has been proposed by Alfano and Crisfield,[26] and the relationship between the normal cohesive traction and normal displacement, δ_n, can be expressed as:

$$\sigma = k_n\delta_n(1-D_n) \tag{8}$$

where $k_n = \sigma_{max}/\delta_n^*$ is the normal cohesive stiffness and σ_{max} is the maximum tensile stress. D_n, the damage parameter, is defined as:

$$D_n = \begin{cases} 0 & \delta_n \leq \delta_n^* \\ \left(\frac{\delta_n-\delta_n^*}{\delta_n}\right)\left(\frac{\delta_n^c}{\delta_n^c-\delta_n^*}\right) & \delta_n^* < \delta_n \leq \delta_n^* \\ 1 & \delta_n > \delta_n^c \end{cases} \tag{9}$$

where δ_n^c is the normal seperation displacement at the completion of debonding, and η is the ratio of δ_n^* and δ_n^c.

For the bilinear CZM model, the fracture energy, G_f, is calculated as:

$$G_f = 2 \times \delta_n^c \times \sigma_{max} \tag{10}$$

NL2SOL is a nonlinear least-squares solution, which has the objective function and optimization algorithm within the program.[22] In NL2SOL, the fracture parameters are taken as the input variable vector, x, and the result of the simulation is y as the output variable vector, respectively. The input and output variable vectors are the nonlinear function relationship:

$$y = g(x) \tag{11}$$

where $x = \{x_i\}$, $I = 1\ldots\ldots N$ and N is the number of input variables, and $y = \{y_j\}$, $j = 1\ldots\ldots M$ and M is the number of output variables.

The residual vector, $R(x)$, is introduced as the function of x and expressed as:

$$R(x) = y - Y = g(x) - Y \tag{12}$$

where Y is the experimental result of WST.

If $R(x) = 0$,the output result of the simulation is in accord with the experimental result. Then, the problem can be transferred to the minimum of the residual sum of squares and the expression is as follows:

$$\min f(x) = \frac{1}{2} R(x)^T R(x) = \frac{1}{2} \sum_{j=1}^{M} r_j(x)^2 \tag{13}$$

where $r_j(x)$ is the residual of j, and $f(x)$ is the residual sum of squares.

The gradient and the Hessian matrices of $f(x)$ are listed as follows:

$$\nabla f(x) = J(x)^T R(x) \tag{14}$$

$$\nabla^2 f(x) = J(x)^T J(x) + \sum_{j=1}^{M} r_j(x) \nabla^2 r_j(x) \tag{15}$$

$$J(x) = R'(x) = \frac{\partial r_j}{\partial x_i} \tag{16}$$

The second-order Taylor series expansion is carried out at the iteration step k (the input variable vector is x_k), and the expression is as follows:

$$f_k(x) = \frac{1}{2} R(x)^T R(x_k) + (x - x_k)^T J(x)^T R(x_k) + \frac{1}{2} (x - x_k)^T [J(x_k)^T J(x_k) + \sum_{j=1}^{M} r_j(x_k) \nabla^2 r_j(x_k)](x - x_k) \tag{17}$$

Therefore, the optimization objective is to calculate the minimum value of the function $f_k(x)$:

$$\nabla f_k(x) = 0 \tag{18}$$

Then, the expression (17) can be converted to the following formula:

$$[J(x_k)^T J(x_k) + \sum_{j=1}^{M} r_j(x_k) \nabla^2 r_j(x_k)](x - x_k) = J(x)^T R(x_k) \tag{19}$$

When it is a small residual problem, the quadratic term $\sum_{j=1}^{M} r_j(x_k) \nabla^2 r_j(x_k)$ can be ignored. The above formula is converted to:

$$J(x_k)^T J(x_k)(x - x_k) = J(x)^T R(x_k) \tag{20}$$

According to the principle of the above optimization method, the minimum residual sum of squares is achieved when the following expression is satisfied:

$$\frac{|\|R_{k+1}(x)\| - \|R_k(x)\||}{\|R_k(x)\|} \leq \varepsilon_A \tag{21}$$

where $R_k(x)$ and $R_{k+1}(x)$ are the residual vectors of steps k and $k + 1$, respectively, and ε_A is the relative residual convergence value.

The steps of the simulation procedure are summarized as follows:

(1) Establish the finite element model and define the cohesive zone model in the commercial finite element software.
(2) Set the initial values and variation ranges of the fracture parameters of CZM based on the experiment.
(3) Carry out the simulation in the finite element software according to the fracture parameters, and record the force–displacement curve.
(4) Compare the curves from the simulation and the experiment, and calculate the residual.
(5) Use the optimization algorithm NL2SOL to calculate the new fracture parameters.
(6) Repeat steps (3)–(5) until the convergence criterion is satisfied and end the calculation.

RESULTS AND DISCUSSION

Determination of the CZM Models

To ensure the accuracy of the inverse simulation, the results of the exponential and bilinear cohesive zone models are compared. The input fracture parameters for the exponential and bilinear CZM models in inverse simulation are listed in Supplementary Table S1. The elastic modulus, E, the surface fracture energy, G_f, and maximum tensile stress, σ_t, are the input optimized parameters in the exponential CZM model, while an extra parameter, η, is added as the input optimized parameters in the bilinear CZM model.

The calculated residual and the relative residual based on the exponential and bilinear CZM model are shown in Figs. 2 and 3, respectively. The solution reaches the convergence criterion for 8 and 11 times iteration, respectively. The minimum residuals of the two models are 3250 and 77.3, respectively. The minimum relative residuals are

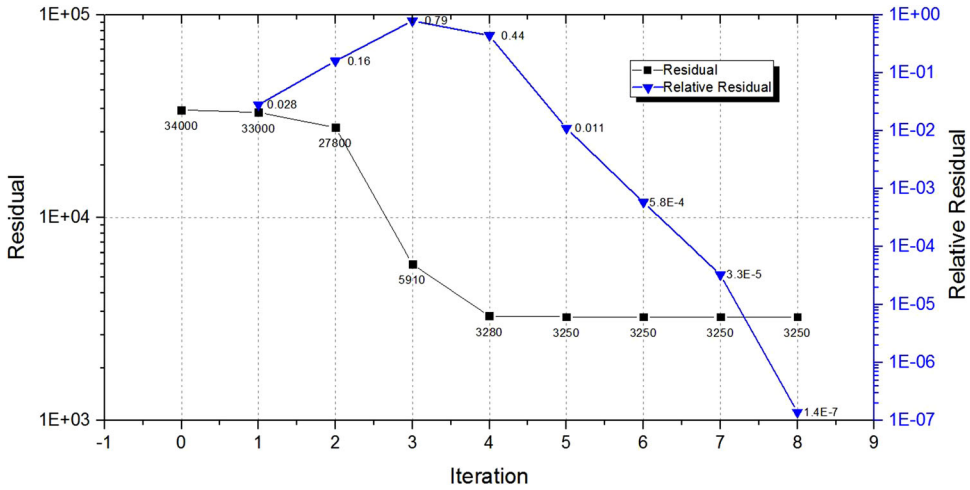

Fig. 2. The residual and relative residual with the iteration steps based on the exponential CZM model.

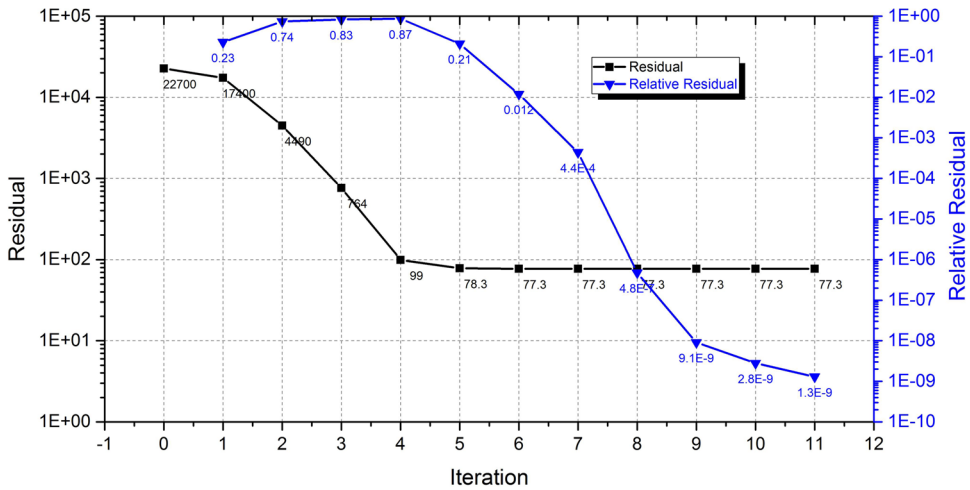

Fig. 3. The residual and relative residual with the iteration steps based on the bilinear CZM model.

1.4E−07 and 1.3E−09, respectively. This indicates that the residual of the bilinear CZM model is significantly lower than that of the exponential CZM model.

The comparison curves between the simulation and experimental results based on the exponential CZM model are set out in Fig. 4. The vertical force–displacement curve calculated according to the initial value is quite different from the experimental and the optimized simulation. The optimized simulation results also greatly differ from the experimental results. It is shown that the optimized simulation results using the exponential CZM model are not suitable.

The force–displacement curves of the simulation and experiment are shown in Supplementary Fig. S1. The vertical force–displacement curve calculated according to the initial value of the input parameters is far from the experiment curve, while the optimization simulation results are consistent with the experimental results. This verifies that the inverse algorithm is feasible to calculate the fracture parameters of refractories by using the bilinear CZM model for the cement-bonded corundum refractories. Therefore, the bilinear CZM model will be adopted in the following section.

Results of Specimens with the Same Formulation

To further confirm the application of the simulation procedure, three specimens with the same recipe and heating temperature are chosen, designated as a#, b# and c#, respectively. The inverse simulations are performed based on the experiment results of the three specimens by the bilinear CZM model. The simulated curves are in accordance with the experimental curves in Fig. 5, and the residuals are similar, namely 8263, 7084 and 7048, respectively.

The fracture parameters of the experiments and the parameters calculated by the inverse simulation for the three specimens are demonstrated in

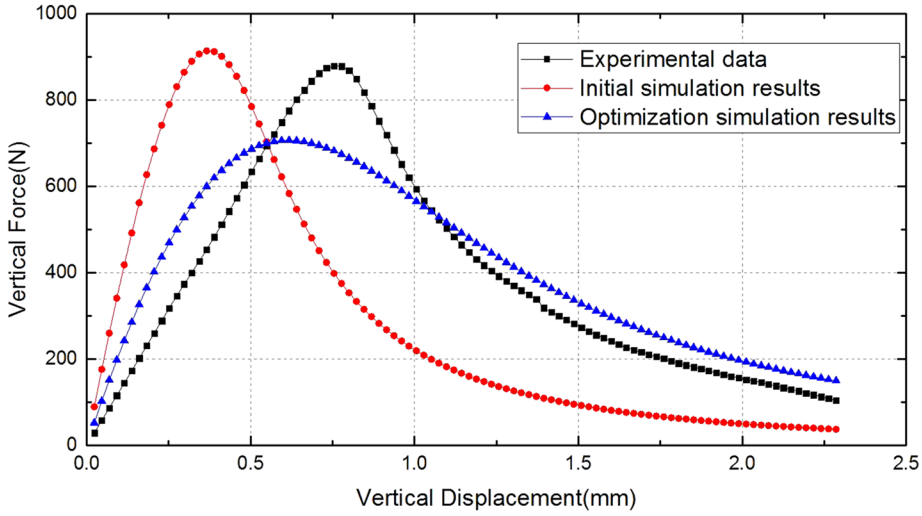

Fig. 4. Force–displacement curves based on the exponential CZM model.

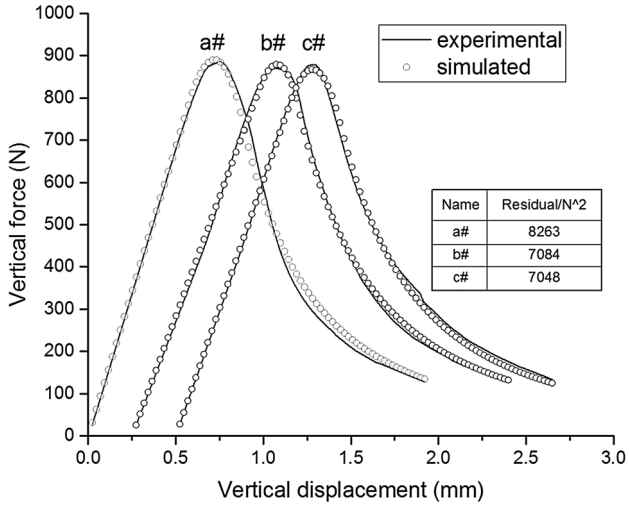

Fig. 5. Experimental and simulated force–displacement curves from the WST (the curves of b# and c# were shifted 0.25 mm to being better distinguish them).

Table I. The mean value of the experimental fracture energy, G_f^E, is equal to 215.64 N/m, and that of simulated G_f^S is 264.01 N/m, which is 22.4% higher than the former. The difference between the G_f^E and G_f^S results from the G_f^E is calculated up to 15% of the maximum load in the experiment as described above. These values of the experimental and simulated for the maximum tensile stress are 8.44 and 6.13 MPa, respectively, illustrating that the latter is 27.4% lower. The discrepancy between σ_{max}^E and σ_{max}^S is owing to the size effect.[27,28] The values of l_{ch}^E and l_{ch}^s are different, evidently derived from the experimental normal stress being considerably larger than the simulated maximum tensile stress.

Results of Specimens with Various Heating Temperatures

Specimens with the same formulation as those in Sec. 3.2 were heated to various temperatures (110°C, 1100°C and 1400°C), and the fracture parameters from experimental and simulated results are compared in Fig. 6, as well as the characteristic length. The differences between the experimental and simulated results present the similar regularity as the previous investigation. The simulated fracture energy is higher than the experiment value, which are about 22.4, 30.8 and 13.7 from 110°C to 1400°C, respectively. In contrast, the maximum tensile stress of simulation is lower by about 27.4%, 28.4% and 1.3% than the experimental results with those temperatures, respectively. After optimization, the increase of the fracture energy and the decrease of strength lead to a large discrepancy of the characteristic length between the experimental and simulated results. On the other hand, the fracture energy and the maximum tensile stress have a minimum at 1100°C and a maximum at 1400°C. According to Refs. 4, 6, and 7 the specimens, in gel states at 110°C, lead to the relatively higher strength. The weak bonding at the interface and the formation of a loose structure cause the lowest strength at 1100°C. Due to the formation of the ceramic phase, the bond force of an interface between the aggregates and the matrix can be strengthened when the temperature rises to 1400°C. Consequently, the fracture energy can be promoted by 48.9% and even the maximum tensile stress increases substantially from 110°C to 1400°C. Based on the analysis of Ref. 29 the cement-bonded corundum refractories present higher brittleness at the high temperature attributed to the low characteristic length, which is adverse to crack propagation.

Table I. Comparison of experimental and simulated results from the WST curves for 3 specimens

		a#	*b*#	*c*#	Mean value	SD
Experimental	Fracture energy G_f^E(N/m)	193.02	229.55	224.36	215.64	15.08
	Max. maximum tensile stress σ_{max}^E(MPa)	8.51	8.36	8.44	8.44	0.05
	l_{ch}^E (mm)	306.02	378.72	363.01	349.25	28.82
Simulated	Fracture energy G_f^S (N/m)	251.84	272.58	267.60	264.01	8.11
	Max maximum tensile stress σ_{max}^S (MPa)	6.22	6.15	6.02	6.13	0.07
	l_{ch}^S (mm)	665.27	736.57	734.94	712.26	31.33

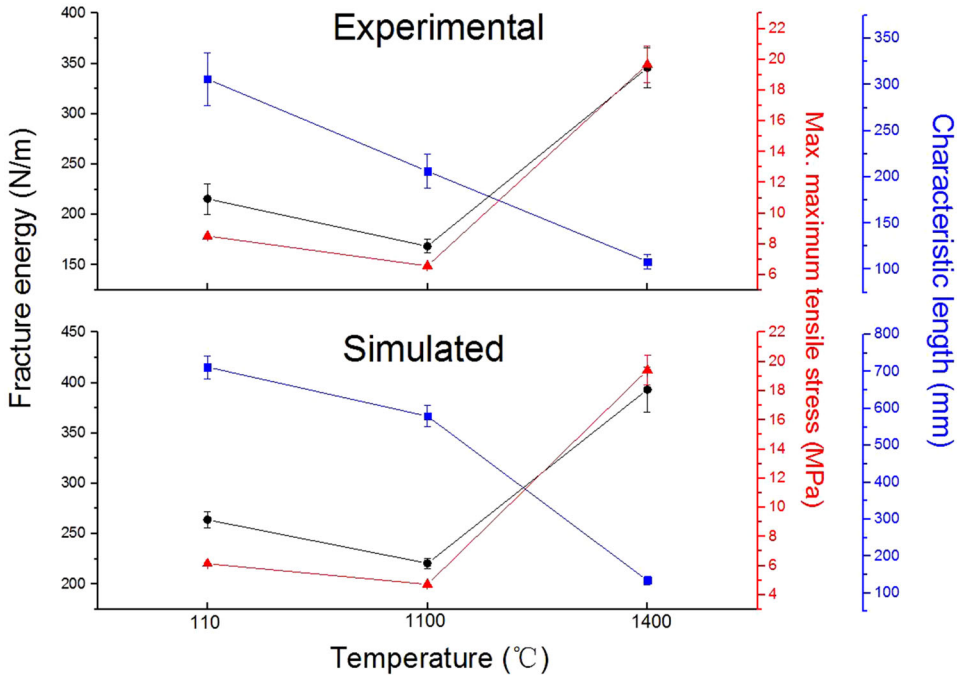

Fig. 6. Experimental and simulated force–displacement curves from the WST for specimens with various heating temperatures.

Results of Specimens with Various Cement Contents

Regarding the fracture mechanical behavior related to the physical properties, the experimental and simulated results for various cement contents (5 wt.%, 10 wt.% and 15 wt.%) at 110°C are shown in Fig. 7. Likewise, the optimized value of fracture energy is larger than the experimental data with the contents of 8.51, 14.61 and 13.59%, respectively. However, that of the maximum tensile stress is smaller than the latter, about 27.4%, 12.6% and 21.9%, respectively. In addition, the fracture energy carries out the tendency of increasing from the content of 5 wt.% to 15 wt.%, which can be explained because the fracture energy of the specimens mainly depends on the hydration intensity of the cement at low temperature.[4] The more the cement content, the higher the hydration intensity, so the fracture energy is proportional to the cement content. The maximum tensile stress increases at the early stage and then decreases with the highest peak at the content of 10 wt.%, which illustrates that more cement content is not favorable to the maximum tensile stress. This can be attributed to the porosity, formed after the cement hydrate decomposes and water vaporizes. The more the cement content, the more water is added, the greater the porosity after drying at 110°C, which causes the structure to lose its load-supporting capability. However, the porosity is beneficial for releasing the thermal stress and prolonging the crack path of propagation. Therefore, the content of 15 wt.% has a higher characteristic length. Moreover, the specimen with the content of 10 wt.% demonstrates a higher brittleness on account of the lowest characteristic length, due to less porosity and higher strength.

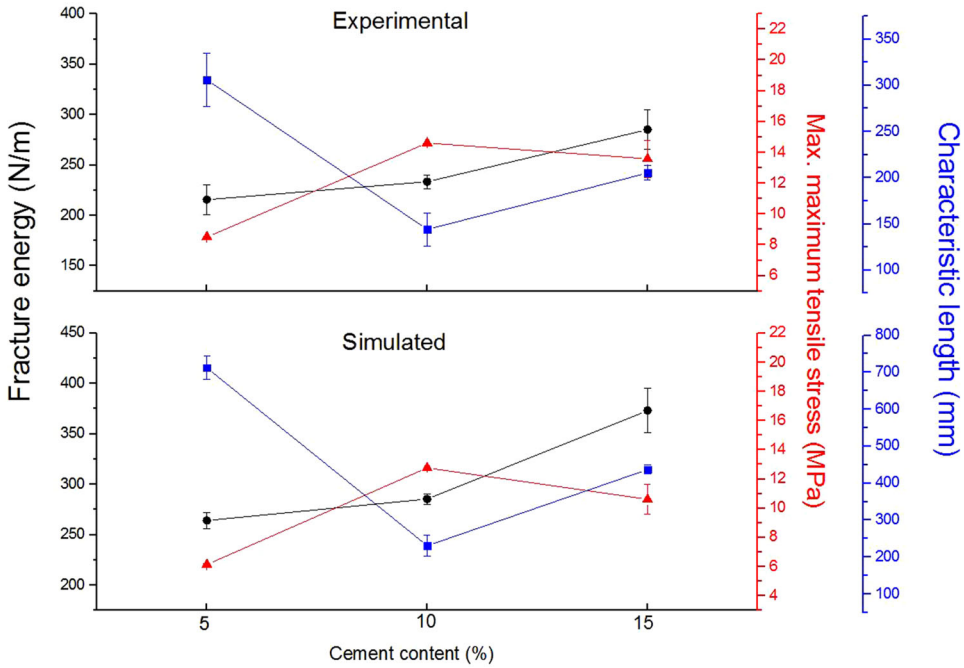

Fig. 7. Experimental and simulated force–displacement curves from the WST for specimens with various cement contents.

CONCLUSION

A new method for determining the fracture parameters for cement-bonded corundum refractories is proposed. To prove the feasibility of the method, several tests with various types of cement-bonded corundum refractory are analyzed. The results show that the bilinear CZM model and the inverse algorithm NL2SOL are well suited to simulate the fracture parameters such as the maximum tensile stress and fracture energy, and a good fit between the simulated and experimental curves is achieved. Additionally, the complete force–displacement curves are computed compared with the experimental curves. The errors of the fracture energy and the maximum tensile stress are approximately 20% and 25%, respectively. Subsequently, the fracture energy and the maximum tensile stress have the minimum at 1100°C and a maximum at 1400°C. The fracture energy carries out the tendency of increasing with the cement content, and the maximum tensile stress increases in the early stage and then decreases with the highest peak at the content of 10 wt.%. The cement-bonded corundum refractory presents higher brittleness at a high temperature (1400°C) or with the cement content of 10 wt.% at 110°C.

ACKNOWLEDGEMENT

The authors are grateful to the National Natural Science Foundation of China (51974211, 51872211 and 51702240) for financial support.

ELECTRONIC SUPPLEMENTARY MATERIAL

The online version of this article (https://doi.org/10.1007/s11837-019-03750-y) contains supplementary material, which is available to authorized users.

REFERENCES

1. V.V. Primachenko, V.V. Martynenko, V.A. Ustichenko, L.A. Babkina, R.M. Fedoruk, I.V. Khonchik, L.K. Savina, L.N. Zolotukhina and A.B. Kovalev, *Proc. UNITECR' 2005*, 27 (2005).
2. W.E. Lee, W. Vieira, S. Zhang, K.G. Ahari, H. Sarpoolaky, and C. Parr, *Int. Mater. Rev.* 46, 145 (2001).
3. C. Parr, L. Bin, B. Valdelievre, C. Wohrmeyer, and B. Touzo, *Proc. ALAFAR Congress* 2004, 10 (2004).
4. Y.E. Hafiane, A. Smith, Y. Abouliatim, T. Chartier, L. Nibou, and J.-P. Bonnet, *J. Eur. Ceram. Soc.* 34, 1017 (2014).
5. W.D. Kingery, *J. Am. Ceram. Soc.* 38, 3 (1955).
6. E.Y. Sako, M.A.L. Braulio, D.H. Milanez, P.O. Brant, and V.C. Pandolfelli, *J. Mater. Process. Tech.* 209, 5552 (2009).
7. N.M. Khalil, *Br. Ceram. Trans.* 103, 37 (2004).
8. J.F. Bartolome, J. Requena, J.S. Moya, M. Li, and F. Guiu, *Acta Mater.* 44, 1361 (1996).
9. D.P.H. Hasselman, *J. Am. Ceram. Soc.* 52, 600 (1969).
10. D.P.H. Hasselman, *J. Am. Ceram. Soc.* 46, 535 (1963).
11. E.K. Tschegg, *Materialprufung.* 333, 38 (1991).
12. A. Hillerborg, *Mater. Struct.* 18, 291 (1985).
13. L.S. Castillo, R. Monte, and A.D.D. Figueiredo, *Constr. Build. Mater.* 192, 731 (2018).
14. J.F. Guan, X.Z. Hu, C.P. Xie, Q.B. Li, and Z.M. Wu, *Theor. Appl. Fract. Mech.* 93, 263 (2018).
15. R.G. Bourdel, A. Alzina, M. Huger, T. Chotard, R. Emler, D. Gruber, and H. Harmuth, *J. Eur. Ceram. Soc.* 33, 913 (2013).

16. T.B. Zhu, Y.W. Li, S.B. Sang, and Z.P. Xie, *J. Eur. Ceram.* 37, 1789 (2017).
17. S. Ribeiro and J.A. Rodrigues, *Ceram. Int.* 36, 263 (2010).
18. D.Y. Miyajia, T. Tonnesenb, and J.A. Rodriguesa, *Ceram. Int.* 40, 15227 (2014).
19. F.H. Wittmann, P.E. Roelfstra, and H. Sadouki, *Mater. Sci. Eng.* 68, 239 (1985).
20. J. Skocek and H. Stang, *Eng. Fract. Mech.* 75, 3173 (2008).
21. Y. Kitsutaka, *J. Eng. Mech.* 123, 44 (1997).
22. J.E. Dennis, D.M. Gay, R.E. Walsh, and A.C.M. Trans, *Math. Soft.* 7, 348 (1981).
23. Y.S. Jenq and S.P. Shahe, *Eng. Fract. Mech.* 21, 1055 (1985).
24. J. Yeoushang and P.S. Surendra, *J. Eng. Mech.* 1111, 227 (1985).
25. X.P. Xu and A. Needleman, *J. Mech. Phys. Solid.* 42, 1397 (1994).
26. G. Alfano and M.A. Crisfield, *Int. J. Numer. Meth. Eng.* 50, 1701 (2001).
27. D.Y. Miyaji, C.Z. Otofuji, A.H.A. Pereira, and J.A. Rodrigues, *Mater. Res.* 18, 250 (2015).
28. S.H. Kwon, Z.F. Zhao, and S.P. Shah, *Cement Concr Res.* 38, 1061 (2008).
29. H. Harmuth and R.C. Bradt, *Interceram Refra. Manua.* 2010, 6 (2010).